

# A Library of Second-Order Models for Synchronous Machines

Olaoluwapo Ajala, *Student Member, IEEE*, Alejandro Domínguez-García, *Member, IEEE*,  
Peter Sauer, *Life Fellow, IEEE*, and Daniel Liberzon, *Fellow, IEEE*

**Abstract**—This paper presents a library of second-order models for synchronous machines that can be utilized in power system dynamic performance analysis and control design tasks. The models have a similar structure to the classical model in that they consist of two dynamic states, the power angle and the angular speed. However, unlike the classical model, the models find applications beyond first swing stability analysis; for example, they can also be utilized in transient stability studies. The models are developed through a systematic reduction of a nineteenth-order model, using singular perturbation techniques, and they are validated by comparing their voltage, frequency, and phase profiles with that of the high-order model and that of the classical model.

**Index Terms**—Synchronous machines, Reduced-order modeling, Singular perturbation analysis.

## I. INTRODUCTION

**D**YNAMIC models of synchronous machines find applications in power system analysis, control design tasks, and education, with each application requiring models that capture dynamical phenomena relevant to the intended use. This has led to the proliferation of synchronous machine models in the literature [1], [2], [3], [4], with varying degrees of complexity, computational cost, and state-space dimension. One such model is the so-called classical model advocated in [5] and [6], a second-order dynamic model that captures the dynamics of the machines phase and angular speed.

Analytically, the classical model is the simplest synchronous machine dynamical model, but it has certain limitations that restrict its applications to first swing stability analysis, i.e. stability analysis for the first second [7], [8], [9]. As a result, if we consider that a power system may be stable in the first swing but unstable in subsequent swings, it is clear that the classical model, though simple, is unreliable for power system tasks extending beyond a one second time interval. For example, the design of a generator synchronization scheme requires a model that captures dynamics of the generator phase, frequency and voltage magnitude over the entire synchronization period. A second-order model such as the classical model should suffice, but the first swing stability constraint could make it inapplicable if the synchronization period exceeds one second. On the other hand, while existing high-order models, such as the two-axis model and the one-axis model [2], [10], are clearly more accurate and therefore very useful for power system simulation, they are also significantly more detailed

and computationally expensive. Consequently, the high-order models are, in general, analytically intractable for such control design tasks. There is therefore a need to develop models that possess the simplicity of the classical model, but also the temporal breadth that it lacks.

The main contribution of this paper is the development of second-order synchronous machine models that, when compared to the classical model, have the same state-space dimension, are significantly more accurate over a long time interval, and are useful for a broader range of applications. Using singular perturbation analysis as our main tool [2], [11], [12], [13], [14], the second-order models presented in this paper are derived by (i) identifying the fastest dynamic states in a high-order model; (ii) developing approximate manifold equations for them, which are algebraic equations; and (iii) replacing the differential equations for these states with the algebraic counterparts.

Our approach to developing the proposed machine models is based on the developments in [2], [14], [15], where zero-order and first-order approximations of manifolds for fast dynamic states are used to develop reduced-order models. In [14], [15], the use of integral manifolds for model order reduction is introduced with some applications presented, and in [2], the technique is used to develop the two-axis model, the one-axis model, and the classical model.

The remainder of the paper is organized as follows. In Section II, we present a synchronous machine and a high-order model that is adopted as the starting point for the development of our reduced order models; we also discuss the classical model. In Section III, we develop a library of second-order models from the high-order model, using singular perturbation analysis. Finally, in Section IV we validate the second-order models developed, using numerical examples, and in Section V we comment on implications of the presented results.

## II. PRELIMINARIES

We begin this section by presenting the high-order model of a synchronous machine adopted in this work. In addition, the time-scale properties of the model are discussed. Afterwards, we introduce the so-called classical model and describe how it can be developed from the high-order model.

### A. High-Order Synchronous Machine Model

The high-order synchronous machine model we describe in this section is based on the developments in [2], [3]. The components included in the model are: (i) three damper

The authors are with the Department of Electrical and Computer Engineering, University of Illinois at Urbana-Champaign, Urbana, IL 61801 USA. E-mail: {ooajala2, aledan, psauer, liberzon}@ILLINOIS.EDU.

windings, (ii) a wound-rotor synchronous machine, (iii) an IEEE type DC1A excitation system [16], and (iv) a Woodward diesel governor (DEGOV1) [17], coupled to a diesel engine, which acts as the prime mover. Next, we provide mathematical expressions that describe the dynamic behavior of these components. [Note that the model is presented utilizing the  $qd0$  transformation, with all parameters and variables scaled, and normalized using the per-unit system].

**Assumption 1.** *The synchronous machine is connected to an electrical network bus through a short transmission line.*

1) *Damper windings model:* Let  $\Phi_{q_2}(t)$  and  $E_{d'}(t)$  denote the flux linkages of two damper windings aligned with the quadrature axis ( $q$ -axis) of the synchronous machine, let  $\Phi_{d_1}(t)$  and  $E_{q'}(t)$  denote the flux linkages of a damper winding and a field winding, respectively, aligned with the direct axis ( $d$ -axis) of the synchronous machine, and let  $I_q$  and  $I_d$  denote the  $q$ -axis and  $d$ -axis components of the stator output current, respectively. Then, the damper winding dynamics can be described as follows:

$$\begin{aligned}\tau_{q''}\dot{\Phi}_{q_2} &= -\Phi_{q_2} - (X_{q'} - X_k)I_q - E_{d'}, \\ \tau_{d''}\dot{\Phi}_{d_1} &= -\Phi_{d_1} - (X_{d'} - X_k)I_d + E_{q'}(t),\end{aligned}\quad (1)$$

and

$$\begin{aligned}\tau_{q'}\dot{E}_{d'} &= -E_{d'} + (X_q - X_{q'})\left(I_q - \frac{X_{q'} - X_{q''}}{(X_{q'} - X_k)^2}(\Phi_{q_2}\right. \\ &\quad \left.+ (X_{q'} - X_k)I_q - E_{d'})\right),\end{aligned}\quad (2)$$

where  $X_k$  denotes the machine leakage reactance,  $X_q$  denotes the machine stator reactance,  $X_{q'}$  and  $X_{d'}$  denote machine transient reactances, and  $X_{q''}$  denotes the machine sub-transient reactance and  $\tau_{q''} = \frac{1}{\omega_0 R_{q_2}}(X_{kq_2} + X_{mq})$ ,  $\tau_{d''} = \frac{1}{\omega_0 R_{d_1}}\left(X_{k_1} + \frac{X_{md}X_{kf}}{X_{md} + X_{kf}}\right)$  and  $\tau_{q'} = \frac{X_{kq_1} + X_{mq}}{\omega_0 R_{q_1}}$  are time constants, with  $X_{kq_2}$ ,  $X_{kd_1}$ ,  $X_{kf}$ ,  $X_{kq_1}$  denoting leakage reactances,  $X_{mq}$  and  $X_{md}$  denoting mutual reactances, and  $R_{q_2}$ ,  $R_{d_1}$ ,  $R_{q_1}$  denoting winding resistances.

2) *Stator windings and network model:* Let  $\Phi_q^{(s)}(t)$  and  $\Phi_d^{(s)}(t)$  denote the  $q$ -axis and  $d$ -axis components of flux linkages for the stator windings, respectively, let  $\Phi_q^{(e)}(t) = -X^{(e)}I_q$ , and  $\Phi_d^{(e)}(t) = -X^{(e)}I_d$  denote the  $q$ -axis and  $d$ -axis components of flux linkages for the electrical line, respectively, let  $\omega^{(s)}(t)$  denote the machine angular speed, in electrical radians per second, and let  $\delta^{(s)}(t)$  denote the power angle of the synchronous machine in electrical radians. At the electrical network bus, let  $V^{(l)}$  and  $\delta^{(l)}$  denote the voltage magnitude, in per unit, and the voltage phase relative to a reference frame rotating at the nominal frequency, in electrical radians, respectively. Let  $V_q^{(l)} := V^{(l)}\cos(\delta^{(s)} - \delta^{(l)})$ ,  $V_d^{(l)} := V^{(l)}\sin(\delta^{(s)} - \delta^{(l)})$ ,  $\Phi_q(t) := \Phi_q^{(s)}(t) + \Phi_q^{(e)}(t)$ ,  $\Phi_d(t) := \Phi_d^{(s)}(t) + \Phi_d^{(e)}(t)$ . Then, the stator winding and network

dynamics are described by:

$$\begin{aligned}\dot{\delta}^{(s)} &= \omega^{(s)}(t) - \omega_0, \\ \frac{1}{\omega_0}\dot{\Phi}_q &= -\frac{\omega^{(s)}(t)}{\omega_0}\Phi_d + V_q^{(l)} + (R_s + R^{(e)})I_q, \\ \frac{1}{\omega_0}\dot{\Phi}_d &= \frac{\omega^{(s)}(t)}{\omega_0}\Phi_q + V_d^{(l)} + (R_s + R^{(e)})I_d, \\ \frac{1}{\omega_0}\dot{\Phi}_q^{(e)} &= R^{(e)}I_q - \frac{\omega^{(s)}(t)}{\omega_0}\Phi_d^{(e)} - V_q^{(s)} + V_q^{(l)}, \\ \frac{1}{\omega_0}\dot{\Phi}_d^{(e)} &= R^{(e)}I_d + \frac{\omega^{(s)}(t)}{\omega_0}\Phi_q^{(e)} - V_d^{(s)} + V_d^{(l)}, \\ \Phi_q &= -X_{q''}^{(e)}I_q + \frac{X_{q'} - X_{q''}}{X_{q'} - X_k}\Phi_{q_2} - \frac{X_{q''} - X_k}{X_{q'} - X_k}E_{d'}, \\ \Phi_d &= -X_{d''}^{(e)}I_d + \frac{X_{d'} - X_{d''}}{X_{d'} - X_k}\Phi_{d_1} + \frac{X_{d''} - X_k}{X_{d'} - X_k}E_{q'}(t),\end{aligned}\quad (3)$$

where  $X_{q''}^{(e)} := X_{q''} + X^{(e)}$ , and  $X_{d''}^{(e)} := X_{d''} + X^{(e)}$ ,  $X^{(e)}$  denotes the per-phase line reactance,  $X_{d''}$  denotes a machine sub-transient reactance,  $R^{(e)}$  denotes the per-phase line resistance,  $R_s$  denotes the per-phase stator resistance, and  $\omega_0$  denotes the nominal frequency in electrical radians per second.

3) *Excitation system model:* Let  $E_f(t)$  denote the output voltage of the machines excitation system, let  $U_f(t)$  denote the exciter control input, let  $\bar{U}_f(t)$  denote the rate feedback variable of the voltage regulator, and let  $V^{(s)} := \sqrt{(V_q^{(s)})^2 + (V_d^{(s)})^2}$ .

**Assumption 2.** *The effects of magnetic saturation on the machines excitation system are negligible.*

Then, the dynamics of the machines excitation system can be described as follows:

$$\begin{aligned}\tau_{d'}\dot{E}_{q'} &= -E_{q'} - (X_d - X_{d'})\left(I_d - \frac{X_{d'} - X_{d''}}{(X_{d'} - X_k)^2}(\Phi_{d_1}\right. \\ &\quad \left.+ (X_{d'} - X_k)I_d - E_{q'})\right) + E_f, \\ \tau_f\dot{E}_f &= -K_f E_f + U_f, \\ \tau_u\dot{U}_f &= -U_f + K_u\bar{U}_f - \frac{K_u\bar{K}_u}{\bar{\tau}_u}E_f + K_u(V_r^{(s)} - V^{(s)}), \\ \bar{\tau}_u\dot{\bar{U}}_f &= -\bar{U}_f + \frac{\bar{K}_u}{\bar{\tau}_u}E_f,\end{aligned}\quad (4)$$

where  $V_r^{(s)}$  denotes the reference voltage magnitude,  $\tau_{d'} = \frac{X_f}{\omega_0 R_f}$ ,  $\tau_f = \frac{L_f}{K_g}$ ,  $K_f = \frac{\bar{R}_f}{K_g}$ ,  $\bar{\tau}_u = \frac{L_t + L_m}{R_t}$ ,  $\bar{K}_u = \frac{N_{t2} L_m}{N_{t2} R_t}$ ,  $X_d$  denotes the machine stator reactance,  $\tau_u$  denotes the amplifier time constant,  $K_u$  denotes the amplifier gain,  $X_f$  denotes the field winding reactance,  $R_f$  denotes the field winding resistance,  $L_f$  denotes the unsaturated field inductance,  $K_g$  denotes the slope of the unsaturated portion of the exciter saturation curve,  $\bar{R}_f$  denotes the exciter circuit resistance,  $L_t$  and  $L_m$  denote series and magnetizing inductances of the stabilizing transformer, which is used to stabilize the excitation system through voltage feedback [2], respectively,  $R_t$  denotes

the series resistance of a stabilizing transformer, and  $\frac{N_{t2}}{N_{t1}}$  denotes the turns ratio of the stabilizing transformer.

4) *Prime mover and speed governor model*: Let  $T_m(t)$  denote the mechanical torque output of the machine. For the speed governor system, let  $P_{a2}(t)$  denote the output of its actuator, with  $\dot{P}_{a1} = P_{a2}(t)$ , and let  $P_{b2}(t)$  denote the output of its electric control box, with  $\dot{P}_{b1} = P_{b2}(t)$ . Let  $\dot{P}_u = P_{a1}(t) + \tau_4 P_{a2}(t)$  denote the valve position of the diesel engine, which acts as the prime mover. Then, the speed control system of the synchronous machine can be expressed as follows:

$$\begin{aligned} M\dot{\omega}^{(s)} &= T_m - \Phi_d(t)I_q + \Phi_q(t)I_d - \tilde{D}_0\omega^{(s)}, \\ \tau_m\dot{T}_m &= -T_m + P_u, \\ \tau_{a2}\dot{P}_{a2} &= -\frac{1}{\tau_5 + \tau_6} \left( P_{a1}(t) - \kappa (P_{b1}(t) + \tau_3 P_{b2}) \right) - P_{a2}, \\ \tau_2\dot{P}_{b2} &= \frac{1}{\tau_1} \left( \frac{1}{\tilde{D}_0\omega_0} (P_c - P_u) - \frac{1}{\omega_0} (\omega^{(s)} - \omega_0) \right) \\ &\quad - P_{b2} - \frac{1}{\tau_1} P_{b1}(t), \end{aligned} \quad (5)$$

where  $\tau_2, \tau_3, \tau_4, \tau_5$  and  $\tau_6$  denote time constants of the control system,  $\tau_{a2} = \frac{\tau_5\tau_6}{\tau_5 + \tau_6}$ ,  $\kappa$  denotes a controller gain for the actuator,  $P_c$  denotes the power change setting of the machine,  $M$  denotes the inertia of the machine,  $\tilde{D}_0$  denotes the friction and windage damping coefficient of the machine,  $\tau_m$  denotes the time constant of the engine, and  $\tilde{D}_0 = \frac{1}{R_D\omega_0}$ , with  $R_D$  denoting the droop coefficient. [Note that for salient pole machines,  $X_q = X_{q'}$ , so that  $E_{d'}(t) = 0$ , and for round-rotor machines,  $X_q = X_d$ ].

### B. High-Order Model Time-Scale Properties

The following observations are based on standard parameter values obtained from synchronous machine models in [1], [2], [3], [17], and an eigenvalue analysis of these models.

**Observation 1.** *The dynamics of  $\Phi_{q2}, \Phi_{d1}, E_{d'}, \Phi_q, \Phi_d, \Phi_q^{(e)}, \Phi_d^{(e)}, E_{q'}, E_f, U_f, \bar{U}_f, T_m, P_u, P_{a2}, P_{b2}, P_{a1}$  and  $P_{b1}$ , are much faster than those of  $\omega^{(s)}$  and  $\delta^{(s)}$ .*

**Observation 2.** *For  $\epsilon = 0.1$  denoting a constant, the parameters  $R_s, \tau_{q''}, \tau_{q'}$ ,  $\frac{1}{\omega_0}, \tau_f, \tau_u, \bar{\tau}_u, \tau_m, \tau_{a2}, \tau_2, \tau_1, (\tau_5 + \tau_6), \frac{\tau_5\tau_6}{(\tau_5 + \tau_6)}, \frac{1}{\kappa R_D}$  are  $\mathcal{O}(\epsilon)^1$ .*

Based on these observations, the nineteenth-order machine model described by (1)–(5) can be expressed compactly as:

$$\begin{aligned} \dot{\mathbf{x}}(t) &= f(\mathbf{x}(t), \mathbf{z}(t), \epsilon), & \mathbf{x}(0) &= \mathbf{x}^0, \\ \epsilon\dot{\mathbf{z}}(t) &= g(\mathbf{x}(t), \mathbf{z}(t), \epsilon), & \mathbf{z}(0) &= \mathbf{z}^0, \end{aligned} \quad (6)$$

where  $\mathbf{x}(t) = \begin{bmatrix} \delta^{(s)} & \omega^{(s)} \end{bmatrix}^\top$ , and  $\mathbf{z}(t) = \begin{bmatrix} \Phi_q & \Phi_d & E_{d'} & \Phi_{q2} & \Phi_{d1} & \Phi_q^{(e)} & \Phi_d^{(e)} & E_{q'} & E_f & U_f & \bar{U}_f & T_m & P_u & P_{a2} & P_{b2} & P_{a1} & P_{b1} \end{bmatrix}^\top$ . In the remainder of this paper, we refer to the elements of  $\mathbf{z}(t)$  as the fast states, and elements of

$\mathbf{x}(t)$  as the slow states. Other observations, which will prove useful in Sections III-B and III-C are:

**Observation 3.** *The dynamics of  $\Phi_q, \Phi_d, \Phi_q^{(e)}$  and  $\Phi_d^{(e)}$  are much faster than those of  $\Phi_{q2}, \Phi_{d1}, E_{d'}$  and  $E_{q'}$ .*

**Observation 4.** *The dynamics of  $\Phi_{q2}$  and  $\Phi_{d1}$  are much faster than those of  $E_{d'}$  and  $E_{q'}$ .*

### C. Classical Model

The classical model of a synchronous machine is a second-order model whose formulation is based on the following assumptions [18]: (i) the machine can be modeled as a constant magnitude voltage source with a series reactance, (ii) the mechanical rotor angle of the machine can be represented by the angle of the voltage source, (iii) damping can be neglected, and (iv) the machines mechanical power input is constant. Thus, the classical model can be obtained from the high-order model by setting  $\tau_{q''} = 0, \tau_{d''} = 0, \frac{1}{\omega_0} = 0, \frac{\omega^{(s)}(t)}{\omega_0} = 1, R_s = 0, R_e = 0, X_{q'} = X_{d'}, \tau_{q'} = \infty, \tau_{d'} = \infty, \tau_m = \infty$  to give:

$$\begin{aligned} \dot{\delta}^{(s)} &= \omega^{(s)} - \omega_0, \\ M\dot{\omega}^{(s)} &= T_m(0) - \frac{E_0}{X_{d'}^{(e)}} V^{(l)} \sin(\delta^{(s)} - \delta^{(l)}) \\ &\quad - \tilde{D}_0\omega^{(s)}, \end{aligned} \quad (7)$$

where  $E_0 = \sqrt{(E_{q'}(0))^2 + (E_{d'}(0))^2}$  and  $X_{d'}^{(e)} := X_{d'} + X^{(e)}$  denote constants.

## III. A LIBRARY OF SECOND-ORDER MODELS

In this section, a library of dynamic models for synchronous machines are developed from the high-order model presented in Section II-A. By utilizing the time-scale properties described in Section II-B, and singular perturbation analysis, the nineteenth-order machine model is reduced to the elemental model, the damped model, and the semi-damped model. Let

$$R_s^{(e)} := R_s + R^{(e)}, \quad X_q^{(e)} := X_q + X^{(e)}, \quad X_d^{(e)} := X_d + X^{(e)}.$$

**Assumption 3.** *The angular speed of the machine,  $\omega^{(s)}(t)$ , is sufficiently close to the nominal speed of the machine so that  $\frac{\omega^{(s)}(t)}{\omega_0} = 1 + \mathcal{O}(\epsilon)$ .*

### A. The Elemental Model

The elemental model is formulated by replacing the differential equations for the fast states with algebraic counterparts called zero-order approximate manifolds. The formulation of these manifolds is presented in Appendix A.

Substituting the zero-order approximate manifolds in (21) and (22) into (1)–(5), the elemental model is given by:

$$\begin{aligned} \dot{\delta}^{(s)} &= \omega^{(s)} - \omega_0, \\ M\dot{\omega}^{(s)} &= P_r^{(s)} - D_0\omega^{(s)} - R_s^{(e)}(I)^2 + C_r \left( V^{(l)} \right)^2 \\ &\quad - C_k C_r \left( V_r^{(s)} - V^{(s)} \right) V^{(l)} \cos(\delta^{(s)} - \delta^{(l)}) \\ &\quad - C_k \tilde{C}_x \left( V_r^{(s)} - V^{(s)} \right) V^{(l)} \sin(\delta^{(s)} - \delta^{(l)}) \\ &\quad - \frac{C_x}{2} \left( V^{(l)} \right)^2 \sin 2(\delta^{(s)} - \delta^{(l)}), \end{aligned} \quad (8)$$

<sup>1</sup>Consider a positive constant  $\epsilon$ , where  $\epsilon < 1$ , and a function  $f(\epsilon)$ , defined on some subset of the real numbers. We write  $f(\epsilon) = \mathcal{O}(\epsilon^t)$  if and only if there exists a positive real number  $k$ , such that:  $|f(\epsilon)| \leq k\epsilon^t$ , as  $\epsilon \rightarrow 0$ .

where  $C_r$ ,  $C_k$ ,  $\tilde{C}_x$  and  $C_x$  are constants, with  $C_r = \frac{R_s^{(e)}}{(R_s^{(e)})^2 + X_q^{(e)} X_d^{(e)}}$ ,  $C_k = \frac{K_f}{K_f}$ ,  $\tilde{C}_x = \frac{X_q^{(e)}}{(R_s^{(e)})^2 + X_q^{(e)} X_d^{(e)}}$ ,  $C_x = \frac{X_d - X_q}{X_q^{(e)} X_d^{(e)}}$ , and  $P_r^{(s)} = P_c + \bar{D}_0 \omega_0$ ,  $D_0 = \bar{D}_0 + \tilde{D}_0$ , and  $I = \sqrt{(I_q)^2 + (I_d)^2}$ . The dynamic circuit of the elemental model is depicted in Fig. 1. For the special case where  $R_s$  and  $R^{(e)}$  are  $\mathcal{O}(\epsilon)$ , we set  $R_s^{(e)} = 0$ , from where it follows that  $C_r = 0$ , and  $\tilde{C}_x = \frac{1}{X_d^{(e)}}$ .

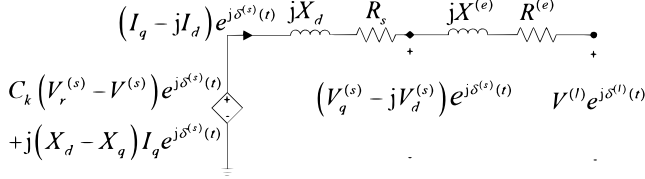


Fig. 1: Dynamic circuit of synchronous machine elemental model.

### B. The Damped Model

The damped model is formulated by replacing (1) and (2) with first-order approximate manifolds, and replacing the differential equations for other fast states with zero-order approximate manifolds. By using a first-order approximation for the damper windings manifolds, the effects of damper windings on the machine response are captured by the resulting reduced model. The following simplifying assumption is employed:

**Assumption 4.** The per-phase line resistance,  $R^{(e)}$  is  $\mathcal{O}(\epsilon)$ .

Starting with the states observed to have the fastest dynamics,  $\Phi_q(t)$ ,  $\Phi_d(t)$ ,  $\Phi_q^{(e)}(t)$  and  $\Phi_d^{(e)}(t)$ , we formulate the zero-order approximate manifolds presented in the first paragraph of Appendix B. Next, for the subsequent fastest states,  $\Phi_{q2}(t)$  and  $\Phi_{d1}(t)$ , which are damper winding states, we derive a first-order approximation of its manifold. Manifolds for  $\Phi_{q2}(t)$  and  $\Phi_{d1}(t)$ , can be expressed as power series in  $\tau_{q''}$  and  $\tau_{d''}$ , respectively, to give:

$$\begin{aligned} \Phi_{q2}(t) &= \Phi_{q2,0}(t) + \tau_{q''}\Phi_{q2,1}(t) + (\tau_{q''})^2\Phi_{q2,2}(t) + \dots, \\ \Phi_{d1}(t) &= \Phi_{d1,0}(t) + \tau_{d''}\Phi_{d1,1}(t) + (\tau_{d''})^2\Phi_{d1,2}(t) + \dots, \end{aligned} \quad (9)$$

where ‘0’ subscripts are used to denote a zero-order approximations, and where first-order approximations are given by:

$$\begin{aligned} \Phi_{q2}(t) &\approx \Phi_{q2,0}(t) + \tau_{q''}\Phi_{q2,1}(t), \\ \Phi_{d1}(t) &\approx \Phi_{d1,0}(t) + \tau_{d''}\Phi_{d1,1}(t). \end{aligned} \quad (10)$$

Expressions for  $\Phi_{q2,0}(t)$ ,  $\Phi_{q2,1}(t)$ ,  $\Phi_{d1,0}(t)$  and  $\Phi_{d1,1}(t)$  are derived using the following steps:

- Substitute (9) into (1) to give:

$$\begin{aligned} \tau_{q''} \frac{d}{dt} (\Phi_{q2,0}(t) + \tau_{q''}\Phi_{q2,1}(t) + \dots) &= -(\Phi_{q2,0}(t) \\ &+ \tau_{q''}\Phi_{q2,1}(t) + \dots) - (X_{q'} - X_k)I_q - E_{d'}(t), \\ \tau_{d''} \frac{d}{dt} (\Phi_{d1,0}(t) + \tau_{d''}\Phi_{d1,1}(t) + \dots) &= -(\Phi_{d1,0}(t) \\ &+ \tau_{d''}\Phi_{d1,1}(t) + \dots) - (X_{d'} - X_k)I_d + E_{q'}(t). \end{aligned} \quad (11)$$

- Using the zero-order approximations in (23), substitute expressions for  $I_q$  and  $I_d$  into (11) and equate the  $(\tau_{q''})^0$  and  $(\tau_{d''})^0$  terms to give:

$$\begin{aligned} \Phi_{q2,0}(t) &= -\frac{X_k^{(e)}}{X_{q'}^{(e)}}E_{d'}(t) - \frac{X_{q'} - X_k}{X_{q'}^{(e)}}V^{(l)} \sin(\delta^{(s)}(t) - \delta^{(l)}), \\ \Phi_{d1,0}(t) &= \frac{X_k^{(e)}}{X_{d'}^{(e)}}E_{q'}(t) + \frac{X_{d'} - X_k}{X_{d'}^{(e)}}V^{(l)} \cos(\delta^{(s)}(t) - \delta^{(l)}), \end{aligned}$$

where  $X_k^{(e)} := X_k + X^{(e)}$ .

- Also equate the  $(\tau_{q''})^1$  and  $(\tau_{d''})^1$  terms to give:

$$\begin{aligned} \Phi_{q2,1}(t) &= -\frac{X_{q'}^{(e)} X_k^{(e)}}{\tau_{q'} (X_{q'}^{(e)})^3} (X_q^{(e)} E_{d'}(t) - (X_q - X_{q'}) V^{(l)} \\ &\cdot \sin(\delta^{(s)}(t) - \delta^{(l)})) + \frac{X_{q'}^{(e)} (X_{q'} - X_k)}{(X_{q'}^{(e)})^2} \dot{V}_d^{(l)}, \\ \Phi_{d1,1}(t) &= \frac{X_{d'}^{(e)} X_k^{(e)}}{\tau_{d'} (X_{d'}^{(e)})^3} (X_d^{(e)} E_{q'}(t) - (X_d - X_{d'}) V^{(l)} \\ &\cdot \cos(\delta^{(s)}(t) - \delta^{(l)})) - \frac{X_{d'}^{(e)} (X_{d'} - X_k)}{(X_{d'}^{(e)})^2} \dot{V}_q^{(l)} \\ &- \frac{X_{d'}^{(e)} X_k^{(e)}}{\tau_{d'} (X_{d'}^{(e)})^2} E_f(t), \end{aligned}$$

where  $\dot{V}_d^{(l)} = V^{(l)} \cos(\delta^{(s)}(t) - \delta^{(l)}) (\dot{\delta}^{(s)}(t) - \dot{\delta}^{(l)}) + \dot{V}^{(l)} \sin(\delta^{(s)}(t) - \delta^{(l)})$ ,  $\dot{V}_q^{(l)} = \dot{V}^{(l)} \cos(\delta^{(s)}(t) - \delta^{(l)}) - V^{(l)} \sin(\delta^{(s)}(t) - \delta^{(l)}) (\dot{\delta}^{(s)}(t) - \dot{\delta}^{(l)})$ , and  $X_{q'}^{(e)} := X_{q'} + X^{(e)}$ . Next, for the damper winding state observed to have the slower dynamics,  $E_{d'}(t)$ , we derive a first-order approximation of its manifold. A manifold for  $E_{d'}(t)$  can be expressed as a power series in  $\tau_{q'}$  to give:

$$E_{d'}(t) = E_{d',0}(t) + \tau_{q'} E_{d',1}(t) + (\tau_{q'})^2 E_{d',2}(t) + \dots, \quad (12)$$

from where it follows that a first-order approximation is given by:

$$E_{d'}(t) \approx E_{d',0}(t) + \tau_{q'} E_{d',1}(t). \quad (13)$$

Expressions for  $E_{d',0}(t)$  and  $E_{d',1}(t)$  can be derived using the following steps:

- Substitute (10) and (12) into (2) to give:

$$\begin{aligned} \tau_{q'} \frac{d}{dt} (E_{d',0}(t) + \tau_{q'} E_{d',1}(t) + \dots) &= \\ &- (E_{d',0}(t) + \tau_{q'} E_{d',1}(t) + \dots) \\ &+ (X_q - X_{q'}) \left( I_q - \frac{X_{q'} (X_{q'} - X_{q''})}{X_{q''} (X_{q'} - X_k)} \tau_{q''} \Phi_{q2,1}(t) \right). \end{aligned} \quad (14)$$

- Using the zero-order approximations in (23), substitute the expressions for  $I_q$  and  $\Phi_{q2,1}(t)$ , into (14), and equate the  $(\tau_{q'})^0$  terms to give:

$$E_{d',0}(t) = \frac{X_q - X_{q'}}{X_q^{(e)}} V^{(l)} \sin(\delta^{(s)}(t) - \delta^{(l)}) - \frac{N_q}{D_q} \dot{V}_d^{(l)},$$

$$\text{where } N_q = \tau_{q'} \tau_{q''} X_{q'}^{(e)} X_k^{(e)} (X_q - X_{q'}) (X_{q'} - X_{q''}) \cdot (X_{q'} - X_k), \quad D_q = \tau_{q'} X_q^{(e)} (X_q^{(e)})^2 (X_{q'} - X_k)^2 - \tau_{q''} X_q^{(e)} (X_k^{(e)})^2 (X_q - X_{q'}) (X_{q'} - X_{q''}).$$

- Also equate the  $(\tau_{q'})^1$  terms to give:

$$E_{d',1}(t) = -\frac{N_{q'}}{\tilde{D}_q} \dot{V}_d^{(l)} + \mathcal{O}(\tau_{q'}),$$

$$\text{where } N_{q'} = \tau_{q'} (X_q^{(e)})^3 (X_q - X_{q'}) (X_{q'} - X_k)^2 \quad \text{and} \\ \tilde{D}_q = X_q^{(e)} D_q.$$

Finally, for other states observed to have fast dynamics, i.e.,  $E_{q'}$ ,  $E_f$ ,  $U_f$ ,  $\bar{U}_f$ ,  $T_m$ ,  $P_u$ ,  $P_{a2}$ ,  $P_{b2}$ ,  $P_{a1}$ , and  $P_{b1}$ , zero-order manifolds are derived as described in the second paragraph of Appendix B.

Substituting the first-order approximate manifolds in (10), (13), and the zero-order approximate manifolds in (21), (23), and (24) into (1)–(5), and setting  $\mathcal{O}((\tau_{q'})^2)$  terms to zero, the damped model for a non-salient pole machine is given by:

$$\dot{\delta}^{(s)} = \omega^{(s)} - \omega_0,$$

$$\begin{aligned} M\dot{\omega}^{(s)} &= P_r^{(s)} - D_0\omega^{(s)} - \frac{C_x}{2} (V^{(l)})^2 \sin 2(\delta^{(s)} - \delta^{(l)}) \\ &\quad - \frac{C_k}{X_d^{(e)}} (V_r^{(s)} - V^{(s)}) V^{(l)} \sin(\delta^{(s)} - \delta^{(l)}) \\ &\quad - C_q (V^{(l)})^2 \cos^2(\delta^{(s)} - \delta^{(l)}) (\dot{\delta}^{(s)} - \dot{\delta}^{(l)}) \\ &\quad - C_d (V^{(l)})^2 \sin^2(\delta^{(s)} - \delta^{(l)}) (\dot{\delta}^{(s)} - \dot{\delta}^{(l)}) \\ &\quad - \frac{(C_q - C_d)}{2} \dot{V}^{(l)} V^{(l)} \sin 2(\delta^{(s)} - \delta^{(l)}), \end{aligned} \quad (15)$$

where  $C_k$ ,  $C_x$ ,  $C_q$ , and  $C_d$  are constants,  $C_k = \frac{K_m}{K_f}$ ,  $C_x = \frac{(X_d - X_q)}{X_q^{(e)} X_d^{(e)}}$ ,  $C_q = C_{q''} + (C_{q'} + \tilde{C}_{q''})^2 \tilde{C}_q$ , with  $C_{q''} = \frac{\tau_{q''} (X_{q'} - X_{q''})}{(X_{q'}^{(e)})^2}$ ,  $\tilde{C}_q = \frac{(X_q - X_{q'})}{D_q}$ ,  $C_{q'} = \tau_{q'} X_{q'}^{(e)} (X_{q'} - X_k)$ ,  $\tilde{C}_{q''} = \frac{\tau_{q''} X_q^{(e)} X_k^{(e)} (X_{q'} - X_{q''})}{X_{q'}^{(e)}}$ ,

and  $C_d = C_{d''} + (C_{d'} + \tilde{C}_{d''}) \tilde{C}_{d'} \tilde{C}_d$ , with  $C_{d''} = \frac{\tau_{d''} (X_{d'} - X_{d''})}{(X_{d'}^{(e)})^2}$ ,  $\tilde{C}_d = \frac{(X_d - X_{d'})}{D_d}$ ,  $C_{d'} = \tau_{d'} X_{d'}^{(e)} (X_{d'} - X_k)$ ,  $\tilde{C}_{d''} = \frac{\tau_{d''} X_d^{(e)} X_k^{(e)} (X_{d'} - X_{d''})}{X_{d'}^{(e)}}$ . The

dynamic circuit of the damped model is depicted in Fig. 2, with  $\dot{V}_d^{(l)} = V^{(l)} \cos(\delta^{(s)}(t) - \delta^{(l)}) (\dot{\delta}^{(s)}(t) - \dot{\delta}^{(l)}) + \dot{V}^{(l)} \sin(\delta^{(s)}(t) - \delta^{(l)})$ ,  $\dot{V}_q^{(l)} = \dot{V}^{(l)} \cos(\delta^{(s)}(t) - \delta^{(l)}) - V^{(l)} \sin(\delta^{(s)}(t) - \delta^{(l)}) (\dot{\delta}^{(s)}(t) - \dot{\delta}^{(l)})$ . Note that for salient pole machines,  $\tilde{C}_q = 0$ , whereas for round-rotor machines,  $C_x = 0$ .

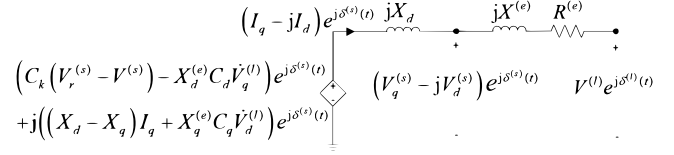


Fig. 2: Dynamic circuit of synchronous machine damped model.

### C. The Semi-Damped Model

The semi-damped model is developed by replacing (2) with a first-order approximate manifold, and replacing the differential equations for other fast states with zero-order approximate manifolds. In salient-pole machines, only one damper winding is aligned with the  $q$ -axis, and the damper winding represented by (2) is typically excluded [3]. Due to this reason, the semi-damped model is only applicable to round-rotor machines.

Starting with fastest states  $\Phi_q(t)$ ,  $\Phi_d(t)$ ,  $\Phi_q^{(e)}(t)$ ,  $\Phi_d^{(e)}(t)$ ,  $\Phi_{q2}(t)$  and  $\Phi_{d1}(t)$ , we develop the zero-order approximate manifolds presented in the first paragraph of Appendix C. Next, we derive a first-order approximate manifold for  $E_{d'}(t)$  having the form

$$E_{d'}(t) \approx E_{d',0}(t) + \tau_{q'} E_{d',1}(t). \quad (16)$$

Substituting the expression for  $\Phi_{q2,0}(t)$  in (25), and the power series expansion in (12) into (2), it follows that:

$$\begin{aligned} \tau_{q'} \frac{d}{dt} (E_{d',0}(t) + \tau_{q'} E_{d',1}(t) + \dots) &= \\ &= (E_{d',0}(t) + \tau_{q'} E_{d',1}(t) + \dots) \frac{X_q^{(e)}}{X_{q'}^{(e)}} \\ &+ \frac{X_q - X_{q'}}{X_{q'}^{(e)}} V^{(l)} \sin(\delta^{(s)}(t) - \delta^{(l)}). \end{aligned} \quad (17)$$

Equating the  $(\tau_{q'})^0$  terms in (17), we have that:

$$E_{d',0}(t) = \frac{X_q - X_{q'}}{X_{q'}^{(e)}} V^{(l)} \sin(\delta^{(s)}(t) - \delta^{(l)}), \quad (18)$$

and equating the  $(\tau_{q'})^1$  terms, we have that:

$$E_{d',1}(t) = -\frac{X_q^{(e)} (X_q - X_{q'})}{(X_q^{(e)})^2} \dot{V}_d^{(l)}, \quad (19)$$

where  $\dot{V}_d^{(l)} = V^{(l)} \cos(\delta^{(s)}(t) - \delta^{(l)}) (\dot{\delta}^{(s)}(t) - \dot{\delta}^{(l)}) + \dot{V}^{(l)} \sin(\delta^{(s)}(t) - \delta^{(l)})$ . Finally, for other states observed to have fast dynamics, i.e.,  $E_{q'}$ ,  $E_f$ ,  $U_f$ ,  $\bar{U}_f$ ,  $T_m$ ,  $P_u$ ,  $P_{a2}$ ,  $P_{b2}$ ,  $P_{a1}$  and  $P_{b1}$ , zero-order approximate manifolds are derived as described in the second paragraph of Appendix C.

Substituting the zero-order approximate manifolds in (21), (25), (26), and the first-order approximate manifold in (16) into (1)–(5), the semi-damped model is given by:

$$\begin{aligned} \dot{\delta}^{(s)} &= \omega^{(s)} - \omega_0, \\ M\dot{\omega}^{(s)} &= P_r^{(s)} - D_0\omega^{(s)} - \frac{\tilde{C}_{q'}}{2}\dot{V}^{(l)}V^{(l)}\sin 2\left(\delta^{(s)} - \delta^{(l)}\right) \\ &\quad - \tilde{C}_{q'}\left(V^{(l)}\right)^2\cos^2\left(\delta^{(s)} - \delta^{(l)}\right)\left(\dot{\delta}^{(s)} - \dot{\delta}^{(l)}\right) \\ &\quad - \frac{C_k}{X_d^{(e)}}\left(V_r^{(s)} - V^{(s)}\right)V^{(l)}\sin\left(\delta^{(s)} - \delta^{(l)}\right), \end{aligned} \quad (20)$$

where  $C_k$  and  $\tilde{C}_{q'}$  are constants, with  $C_k = \frac{K_m}{K_f}$ , and  $\tilde{C}_{q'} = \frac{\tau_{q'}(X_q - X_{q'})}{(X_q^{(e)})^2}$ . The dynamic circuit of the semi-damped model is depicted in Fig. 3, with  $\dot{V}_d^{(l)} = V^{(l)}\cos\left(\delta^{(s)}(t) - \delta^{(l)}\right)\left(\dot{\delta}^{(s)}(t) - \dot{\delta}^{(l)}\right) + \dot{V}^{(l)}\sin\left(\delta^{(s)}(t) - \delta^{(l)}\right)$ .

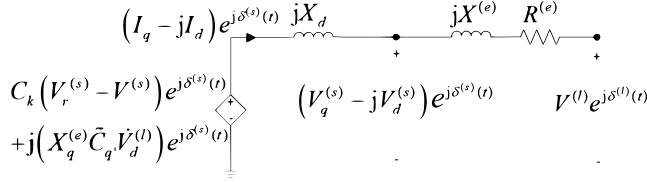


Fig. 3: Dynamic circuit of synchronous machine semi-damped model.

#### IV. NUMERICAL VALIDATION

In this section, simulation results comparing the high-order model, the classical model, the elemental model, the semi-damped model, and the damped model, of a round-rotor synchronous machine, are presented. We consider a two-bus power system with a synchronous machine connected to a constant power load through a short electrical transmission line. See Fig. 4 for a one-line diagram, and Table II for the system parameters.

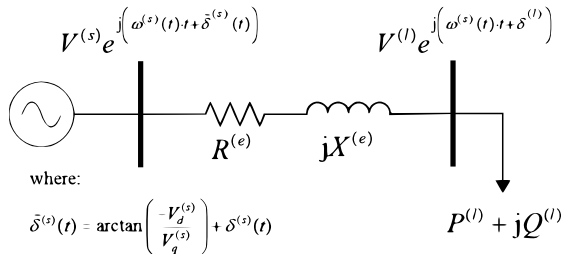


Fig. 4: One line diagram of a power system with a synchronous machine connected to a constant power load through a short transmission line.

##### A. Case 1

This case is used to highlight the high-fidelity of the second-order models in comparison to the classical model, and we

consider the system response to an increase in real power demand by the load. A stable equilibrium point of the high-order model is chosen as the common initial condition for all the models. The real power demand by the load is increased from 0.05 [pu] to 0.25 [pu] at time  $t = 30$  [s], and the reference voltage magnitude  $V_r^{(s)}$  is changed at time  $t = 30$  [s] to keep the bus voltage magnitude at  $V^{(l)} = 1$  [pu]. Numerical results are depicted in Fig. 5, and they show that the elemental model, the semi-damped model and the damped model have an overall better accuracy than the classical model, and that after one second, the error of the classical model response increases exponentially.

##### B. Case 2

This case is used to compare the fidelity of the elemental model, the semi-damped model and the damped model. The machine whose parameters are described in Table II is employed. The real power demand by the load is increased from 0.05 [pu] to 0.25 [pu] at time  $t = 30$  [s], from 0.25 [pu] to 0.35 [pu] at time  $t = 1530$  [s], from 0.35 [pu] to 0.3 [pu] at time  $t = 3030$  [s], and from 0.3 [pu] to 0.15 [pu] at time  $t = 4530$  [s]. For each load change, the reference voltage magnitude  $V_r^{(s)}$  is changed to keep the bus voltage magnitude at  $V^{(l)} = 1$  [pu]. The root mean square errors of the models, relative to the high-order model, are outlined in Table I, and numerical results are presented in Figs. 6.

TABLE I: Root Mean Square Error (RMSE)

	$\omega^{(s)}$	$V^{(s)}$	$\delta^{(s)}$
damped model	2.9093[rpm]	0.0042 [pu]	1065.6 [deg]
semi-damped model	2.9093[rpm]	0.0042 [pu]	1065.6 [deg]
elemental model	80.753[rpm]	0.0042 [pu]	1065.6 [deg]

The RMSE results show that although the elemental model, the semi-damped model and the damped model match in accuracy for machine voltage magnitude response, the damped model and the semi-damped model have a higher accuracy for machine angular frequency response.

#### V. CONCLUDING REMARKS

In this paper, we introduced a library of second-order synchronous machine models, comprising of the elemental model, the damped model, and the semi-damped model. We also showed how these models, and the so-called classical model, can be derived from a high-order machine model. While the classical model is obtained by identifying small and large parameters in the high-order model, and setting them to zero and infinity, respectively, the library of second-order models are obtained by identifying fast and slow states in the high-order model, and replacing differential equations for the fast states with algebraic counterparts, referred to as approximate manifolds (zero-order or first-order). The library of second-order models were validated by comparing their responses to those of a high-order model, and the classical model, for given test cases.

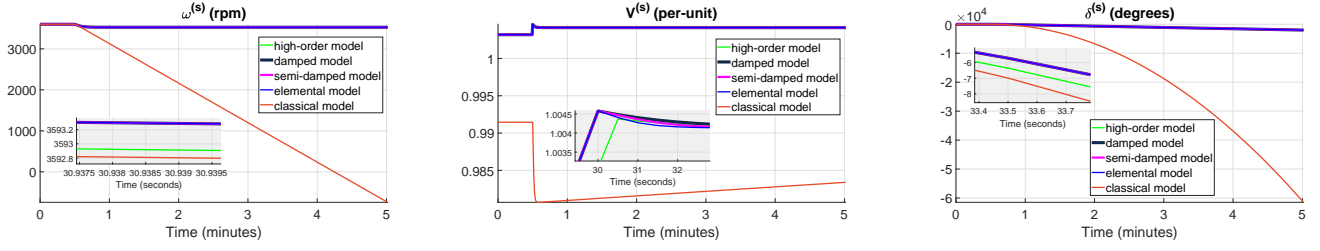


Fig. 5: Case 1 numerical results: machine angular frequency, voltage magnitude and phase.

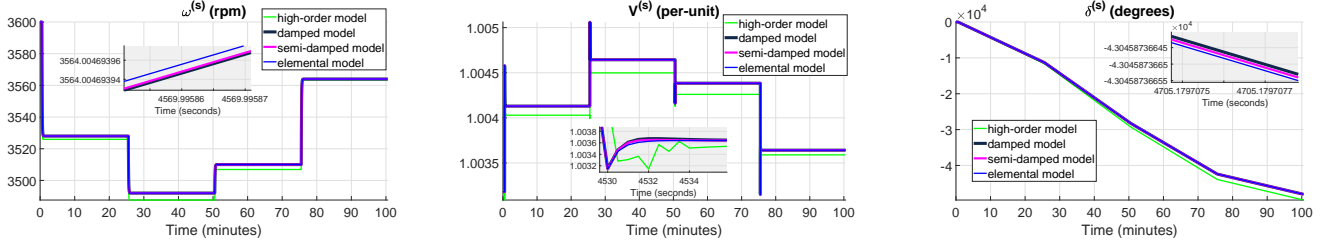


Fig. 6: Case 2 numerical results: machine angular frequency, voltage magnitude and phase.

TABLE II: System parameters for a salient pole synchronous machine

	parameter	value
Damper windings	$\tau_{q''}$	0.9453 [s]
	$\tau_{d''}$	0.042 [s]
	$\tau_{q'}$	3.6123 [s]
	$X_{q''}$	0.2388 [pu]
	$X_{q'}$	0.7299 [pu]
	$X_q$	1.7997 [pu]
	$X_k$	0.19 [pu]
Stator windings	$\omega_0$	376.99 [rad/s]
	$R_s$	0.003 [pu]
	$X_{d''}$	0.24 [pu]
	$X_{d'}$	0.32 [pu]
	$X_d$	1.7997 [pu]
IEEE DC1A exciter	$\tau_{d'}$	5.0141 [s]
	$\tau_f$	$1 \times 10^{-8}$ [s]
	$\tau_u$	0.002 [s]
	$\bar{\tau}_u$	$1 \times 10^{-12}$ [s]
	$X_d$	1.7997 [pu]
	$K_f$	1 [pu]
	$\bar{K}_u$	0 [s]
DEGOV1 speed governor	$\tau_1$	$1 \times 10^{-4}$ [s]
	$\tau_2$	0 [s]
	$\tau_3$	0.5001 [s]
	$\tau_4$	$25 \times 10^{-3}$ [s]
	$\tau_5$	$9 \times 10^{-4}$ [s]
	$\tau_6$	$5.74 \times 10^{-3}$ [s]
	$\tau_m$	$24 \times 10^{-3}$ [s]
	$\kappa$	10
	$P_r^{(s)}$	0 [pu]
	$M$	0.1188 [s <sup>2</sup> ]
$\bar{D}_0$	$2.5825 \times 10^{-7}$ [s/rad]	
$\bar{D}_0$	0.0531 [s/rad]	
Transmission line	$R^{(e)}$	0.004 [pu]
	$X^{(e)}$	0.0595 [pu]

## APPENDIX

In this section, we present the zero-order approximate manifolds that we formulated for the fast states identified in Sec. II-B. These manifolds are used in our formulation of the elemental model, the damped model, and the semi-damped

model. The following zero-order approximate manifolds are common to the elemental model, the damped model, and the semi-damped model.

$$E_{f,0}(t) = \frac{K_u (V_r^{(s)} - V^{(s)})}{K_f}, \quad T_{m,0}(t) = P_{u,0}(t),$$

$$P_{u,0}(t) = P_c - \bar{D}_0 (\omega^{(s)}(t) - \omega_0), \quad P_{b1,0}(t) = 0, \quad (21)$$

$$P_{b2,0}(t) = 0, \quad P_{a1,0}(t) = 0, \quad P_{a2,0}(t) = 0,$$

$$U_{f,0}(t) = K_f E_{f,0}(t), \quad \bar{U}_{f,0}(t) = \frac{\bar{K}_u}{\bar{\tau}_u} E_{f,0}(t),$$

where '0' subscripts are used to denote a zero-order approximation.

### A. The Elemental Model

In order to formulate the elemental model, zero-order manifolds were developed by setting  $\tau_{d''}$ ,  $\tau_{d'}$  and all  $\mathcal{O}(\epsilon)$  parameters in (6) to zero to give (21) and:

$$\Phi_{q,0}^{(e)}(t) = -X^{(e)} I_q,$$

$$\Phi_{d,0}^{(e)}(t) = -X^{(e)} I_d,$$

$$E_{q',0}(t) = -(X_d - X_{d'}) I_d + E_{f,0}(t),$$

$$E_{d',0}(t) = (X_q - X_{q'}) I_q,$$

$$\Phi_{q2,0}(t) = -(X_q - X_k) I_q, \quad (22)$$

$$\Phi_{d1,0}(t) = -(X_d - X_k) I_d + E_{f,0}(t),$$

$$\Phi_{q,0}(t) = -R_s^{(e)} I_d - V^{(l)} \sin(\delta^{(s)}(t) - \delta^{(l)}),$$

$$\Phi_{d,0}(t) = R_s^{(e)} I_q + V^{(l)} \cos(\delta^{(s)}(t) - \delta^{(l)}).$$

The output voltage is described by:  $V_q^{(s)} = R^{(e)} I_q + X^{(e)} I_d + V^{(l)} \cos(\delta^{(s)}(t) - \delta^{(l)})$ ,  $V_d^{(s)} = R^{(e)} I_d - X^{(e)} I_q + V^{(l)} \sin(\delta^{(s)}(t) - \delta^{(l)})$ , and the output current is described

$$\text{by } I_q = \frac{R_s^{(e)} \left( \frac{\kappa_u (V_r^{(s)} - V^{(s)})}{K_f} \right)}{\left( R_s^{(e)} \right)^2 + X_q^{(e)} X_d^{(e)}} - \frac{R_s^{(e)} \left( V^{(l)} \cos(\delta^{(s)}(t) - \delta^{(l)}) \right)}{\left( R_s^{(e)} \right)^2 + X_q^{(e)} X_d^{(e)}} + \frac{X_d^{(e)} \left( V^{(l)} \sin(\delta^{(s)}(t) - \delta^{(l)}) \right)}{\left( R_s^{(e)} \right)^2 + X_q^{(e)} X_d^{(e)}}, \quad I_d = \frac{X_q^{(e)} \left( \frac{\kappa_u (V_r^{(s)} - V^{(s)})}{K_f} \right)}{\left( R_s^{(e)} \right)^2 + X_q^{(e)} X_d^{(e)}} - \frac{X_q^{(e)} \left( V^{(l)} \cos(\delta^{(s)}(t) - \delta^{(l)}) \right)}{\left( R_s^{(e)} \right)^2 + X_q^{(e)} X_d^{(e)}} - \frac{R_s^{(e)} \left( V^{(l)} \sin(\delta^{(s)}(t) - \delta^{(l)}) \right)}{\left( R_s^{(e)} \right)^2 + X_q^{(e)} X_d^{(e)}}.$$

### B. The Damped Model

In other to formulate the damped model, the following zero-order manifolds were developed by setting  $R_s = 0$ ,  $R^{(e)} = 0$ ,  $\frac{1}{\omega_0} = 0$  and  $\frac{\omega^{(s)}(t)}{\omega_0} = 1$ :

$$\begin{aligned} \Phi_{q,0}(t) &= -V^{(l)} \sin(\delta^{(s)}(t) - \delta^{(l)}), \\ \Phi_{d,0}(t) &= V^{(l)} \cos(\delta^{(s)}(t) - \delta^{(l)}), \\ \Phi_{q,0}^{(e)}(t) &= V_d^{(s)} - V^{(l)} \sin(\delta^{(s)}(t) - \delta^{(l)}), \\ \Phi_{d,0}^{(e)}(t) &= -V_q^{(s)} + V^{(l)} \cos(\delta^{(s)}(t) - \delta^{(l)}), \end{aligned} \quad (23)$$

from where it follows that:  $I_q = \frac{(X_{q'} - X_{q''})}{(X_{q'} - X_k)(X_{q''}^{(e)})} \Phi_{q_2}(t) - \frac{(X_{q'} - X_k)}{(X_{q'} - X_k)(X_{q''}^{(e)})} E_{d'}(t) + \frac{V^{(l)} \sin(\delta^{(s)}(t) - \delta^{(l)})}{X_{q''}^{(e)}}$ , and  $I_d = \frac{(X_{d'} - X_{d''})}{(X_{d'} - X_k)(X_{d''}^{(e)})} \Phi_{d_1}(t) + \frac{(X_{d''} - X_k)}{(X_{d'} - X_k)(X_{d''}^{(e)})} E_{q'}(t) - \frac{V^{(l)} \cos(\delta^{(s)}(t) - \delta^{(l)})}{X_{d''}^{(e)}}$ .

A second set of zero-order manifolds was developed by setting  $\tau_{d'}$ , and all  $\mathcal{O}(\epsilon)$  parameters except  $\tau_{q''}$  and  $\tau_{q'}$ , to zero to give (21) and:

$$\begin{aligned} E_{q',0}(t) &= \frac{X_{d'}^{(e)}}{X_d^{(e)}} E_{f,0}(t) - \frac{N_d}{D_d} \dot{V}_q^{(l)} \\ &+ \frac{X_d - X_{d'}}{X_d^{(e)}} V^{(l)} \cos(\delta^{(s)}(t) - \delta^{(l)}), \end{aligned} \quad (24)$$

where  $N_d = \tau_{d'} \tau_{d''} X_{d'}^{(e)} X_k^{(e)} (X_d - X_{d'}) (X_{d'} - X_{d''}) (X_{d'} - X_k)$ , and  $D_d = \tau_{d'} X_d^{(e)} (X_{d'}^{(e)})^2 (X_{d'} - X_k)^2 - \tau_{d''} X_d^{(e)} (X_k^{(e)})^2 (X_d - X_{d'}) (X_{d'} - X_{d''})$ .

### C. The Semi-Damped Model

In other to formulate the semi-damped model, the following zero-order manifolds were developed by setting  $R_s = 0$ ,  $R^{(e)} = 0$ ,  $\frac{1}{\omega_0} = 0$ ,  $\frac{\omega^{(s)}(t)}{\omega_0} = 1$ ,  $\tau_{q''} = 0$  and  $\tau_{d''} = 0$ :

$$\begin{aligned} \Phi_{q,0}(t) &= -V^{(l)} \sin(\delta^{(s)}(t) - \delta^{(l)}), \\ \Phi_{d,0}(t) &= V^{(l)} \cos(\delta^{(s)}(t) - \delta^{(l)}), \\ \Phi_{q,0}^{(e)}(t) &= V_d^{(s)} - V^{(l)} \sin(\delta^{(s)}(t) - \delta^{(l)}), \\ \Phi_{d,0}^{(e)}(t) &= -V_q^{(s)} + V^{(l)} \cos(\delta^{(s)}(t) - \delta^{(l)}), \\ \Phi_{q_2,0}(t) &= -(X_{q'} - X_k) I_q - E_{d'}(t), \\ \Phi_{d_1,0}(t) &= -(X_{d'} - X_k) I_d + E_{q'}(t), \end{aligned} \quad (25)$$

from where it follows that:  $I_q = -\frac{1}{X_{q'}^{(e)}} E_{d'}(t) + \frac{V^{(l)} \sin(\delta^{(s)}(t) - \delta^{(l)})}{X_{q'}^{(e)}}$ ,  $I_d = \frac{1}{X_{d'}^{(e)}} E_{q'}(t) - \frac{V^{(l)} \cos(\delta^{(s)}(t) - \delta^{(l)})}{X_{d'}^{(e)}}$ .

A second set of zero-order manifolds was developed by setting  $\tau_{d''}$ ,  $\tau_{d'}$  and all  $\mathcal{O}(\epsilon)$  parameters except  $\tau_{q'}$  to zero to give (21) and:

$$E_{q',0}(t) = \frac{X_{d'}^{(e)}}{X_d^{(e)}} E_{f,0}(t) + \frac{X_d - X_{d'}}{X_d^{(e)}} V^{(l)} \cos(\delta^{(s)}(t) - \delta^{(l)}), \quad (26)$$

where  $N_d = \tau_{d'} \tau_{d''} X_{d'}^{(e)} X_k^{(e)} (X_d - X_{d'}) (X_{d'} - X_{d''}) (X_{d'} - X_k)$ , and  $D_d = \tau_{d'} X_d^{(e)} (X_{d'}^{(e)})^2 (X_{d'} - X_k)^2 - \tau_{d''} X_d^{(e)} (X_k^{(e)})^2 (X_d - X_{d'}) (X_{d'} - X_{d''})$ .

### REFERENCES

- [1] P. Kundur, N. J. Balu, and M. G. Lauby, *Power system stability and control*. McGraw-Hill, 1994.
- [2] P. Sauer and A. Pai, *Power System Dynamics and Stability*. Stipes Publishing L.L.C., 2006.
- [3] P. Krause, O. Wasynczuk, S. Sudhoff, and S. Pekarek, *Analysis of Electric Machinery and Drive Systems*, ser. IEEE Press Series on Power Engineering. Wiley, 2013.
- [4] L. Wang, J. Jatskevich, and H. W. Dommel, "Re-examination of synchronous machine modeling techniques for electromagnetic transient simulations," *IEEE Transactions on Power Systems*, vol. 22, no. 3, pp. 1221–1230, Aug. 2007.
- [5] S. Crary, *Power System Stability: Transient stability*, ser. General Electric series. John Wiley, 1947.
- [6] E. Kimbark, *Power Systems Stability. Vol. 3. Synchronous Machines*. Wiley, 1956.
- [7] A. Pai, *Energy Function Analysis for Power System Stability*, ser. Power Electronics and Power Systems. Springer, Boston, MA, 1989.
- [8] P. M. Anderson and A. A. Fouad, *Power system control and stability*, ser. IEEE Press power engineering series. IEEE Press, 2003.
- [9] S. Y. Caliskan and P. Tabuada, "Uses and abuses of the swing equation model," in *Proc. of IEEE Conference on Decision and Control (CDC)*, Dec 2015, pp. 6662–6667.
- [10] T. Weckesser, H. Jhannsson, and J. stergaard, "Impact of model detail of synchronous machines on real-time transient stability assessment," in *Proc. of the IREP Symposium Bulk Power System Dynamics and Control - IX Optimization, Security and Control of the Emerging Power Grid*, Aug 2013, pp. 1–9.
- [11] P. Kokotović, H. K. Khalil, and J. O'Reilly, *Singular Perturbation Methods in Control: Analysis and Design*, ser. Classics in Applied Mathematics. Society for Industrial and Applied Mathematics, 1986.
- [12] H. K. Khalil, *Nonlinear Systems*. Pearson Education, Limited, 2013.
- [13] J. H. Chow, *Time-Scale Modeling of Dynamic Networks with Applications to Power Systems*, B. A.V. and T. M., Eds. Springer, 1982.
- [14] P. W. Sauer, S. Ahmed-Zaid, and P. V. Kokotovic, "An integral manifold approach to reduced order dynamic modeling of synchronous machines," *IEEE Transactions on Power Systems*, vol. 3, no. 1, pp. 17–23, Feb. 1988.
- [15] P. V. Kokotovic and P. W. Sauer, "Integral manifold as a tool for reduced-order modeling of nonlinear systems: A synchronous machine case study," *IEEE Transactions on Circuits and Systems*, vol. 36, no. 3, pp. 403–410, Mar. 1989.
- [16] "IEEE Recommended Practice for Excitation System Models for Power System Stability Studies," *IEEE Std 421.5-2016 (Revision of IEEE Std 421.5-2005)*, pp. 1–207, Aug. 2016.
- [17] PowerWorld corporation. (2017) Woodward diesel governor model. [Online]. Available: <https://www.powerworld.com>
- [18] A. Fouad and V. Vittal, *Power System Transient Stability Analysis Using the Transient Energy Function Method*. Prentice Hall, 1992.